ORIGINAL RESEARCH

Identification of a Necroptosis-Related Prognostic Index and Associated Regulatory Axis in Kidney Renal Clear Cell Carcinoma

Yong Luo [1], Guian Zhang[2]

[1]Department of Urology, the Second People's Hospital of Foshan, Affiliated Foshan Hospital of Southern Medical University, Foshan, 528000, People's Republic of China; [2]School of Medicine, South China University of Technology, Guangzhou, 510006, People's Republic of China

Correspondence: Yong Luo, Department of Urology, the Second People's Hospital of Foshan, Affiliated Foshan Hospital of Southern Medical University, 78 Weiguo Road, Foshan, 528000, People's Republic of China, Tel +86-15625093895, Fax +86-0757-88032009, Email luomou5@outlook.com; Guian Zhang, School of Medicine, South China University of Technology, Guangzhou, 510006, People's Republic of China, Tel +86-13246808932, Email machfine@gmail.com

Background: Kidney renal clear cell carcinoma (KIRC) is one of the most common aggressive malignancies in the genitourinary system with the high degree of immune infiltration. However, the role of necroptosis-related genes in the immune infiltration of KIRC and the impact on overall survival have not been adequately studied.

Methods: Differentially expressed necroptosis-related genes were identified based on The Cancer Genome Atlas (TCGA). Then, we constructed a necroptosis-related prognostic index (NRPI) through Lasso Cox regression analysis. The KIRC patients were divided into NRPI-high and NRPI-low groups by the median. Univariate and multivariate Cox regression analyses were used to determine NRPI as an independent prognostic factor. The role of NRPI was assessed through nomogram, GO/KEGG enrichment analyses, and immune cells infiltration. The efficacy of immunotherapy in KIRC patients was evaluated by TIDE. The immunohistochemistry was performed to verify the difference in protein expression between tumor samples and normal tissues from our hospital.

Results: We found that NRPI-high patients had higher mortality. The multivariate Cox regression between the signature and multiple clinicopathological characteristics proved that NRPI could effectively and independently predict the prognosis of KIRC. The protein expression of three necroptosis-related genes constituting NRPI was significantly different between tumor and normal tissues. NRPI was closely related to immunologically relevant pathways and functions. The tumor microenvironment and immune infiltrating cells showed clear distinctions in NRPI-high and NRPI-low patients. The analysis of clinical treatments found that NRPI-low patients responded better to immunotherapy, while NRPI-high patients were more sensitive to targeted therapy. Furthermore, we identified a lncRNAs/miRNA/mRNA regulatory axis for KIRC.

Conclusion: In general, NRPI was a promising biomarker in predicting the prognosis and responses to treatments in KIRC.

Keywords: kidney renal clear cell carcinoma, necroptosis, prognostic index, immune infiltration, immunotherapy

Introduction

Kidney renal clear cell carcinoma (KIRC) is the most common renal malignancy and constitutes the majority of kidney cancer-related deaths due to its early asymptomatic nature that is difficult to be taken seriously.[1] Despite the positive outcome of some patients after early surgical treatment, recurrence and distant metastases still occur in 25% of patients.[2] Although the advent of targeted therapies and immunotherapy has brought hope to some patients, the overall 5-year survival rate is currently only 12% for patients with advanced disease.[3] At present, treatment regimens such as immunotherapy and targeted therapy are primarily scheduled according to the clinical stage of the patient, without taking into account the different responses of the patients. Therefore, early and accurate identification of patients at high risk and appropriate treatment options are critical for KIRC patients.

Necroptosis is a caspase-independent regulated form of programmed necrosis that depends on the kinase activities of RIPK1, RIPK3, and MLKL.[4] Cells undergoing necroptosis are subject to cell swelling followed by plasma membrane rupture, resulting in the release of cellular contents and exposure to damage-related factors. The impact of necroptosis on tumors is like a double-edged sword. On the one hand, it can induce a strong adaptive immune response to prevent tumor progression, and on the other hand, the inflammatory response generated may also promote tumor progression and metastasis.[5] Seehawer et al[6] found that the necroptotic tumor microenvironment could guide the differentiation of the two major subtypes of liver cancer, namely, hepatocellular carcinoma and intrahepatic cholangiocarcinoma, suggesting that necroptosis played an important role in defining liver cancer subtypes. However, it is unclear whether necroptosis can be used as an effective biological factor to stratify KIRC patients with different risk classes and differentiate patients' responses to treatment. Considering the multiple functions of necroptosis in cancer biology, necroptosis may be a new target for the treatment of KIRC.

In the current study, we performed bioinformatics analysis to investigate the expression profile of necroptosis-related genes and to develop and validate a prognostic index based on necroptosis-related genes in KIRC. Then we explored the role of the prognostic index in immunotherapy and targeted therapy. The immunohistochemical experiment was conducted to validate the expression levels of necroptosis-related genes using clinical samples from our hospital and the potential regulatory axis was constructed for KIRC.

Materials and Methods

Databases and Preprocessing

RNA-seq data and corresponding clinical information of 539 KIRC samples and 72 para-cancer samples were obtained from the TCGA program (https://tcga-data.nci.nih.gov/tcga/, Jan 20th, 2022). The entire TCGA database was randomly divide into a training set and an internal validation set by R package "*caret*". The training set was conducted to construct prognostic index. External validation was engaged in another set, E-MTAB-1980 from the ArrayExpress dataset (https://www.ebi.ac.uk/arrayexpress/experiments/E-MTAB-1980/, Jan 20th, 2022). A predictive nomogram was built by the *rms* package. The network of lncRNA-miRNA-mRNA was analyzed from StarBase (http://starbase.sysu.edu.cn/, Jan 20th, 2022).

Identification of Differentially Expressed Necroptosis-Related Genes

A total of 67 necroptosis-related genes were selected based on previously published article.[7] The differentially expressed analysis of necroptosis-related genes with a P value < 0.05 was identified by *limma* R package. The univariate Cox regression was adopted to determine the necroptosis-related genes with prognostic value. The Venn diagram was depicted by Venn R package. A protein-protein interaction (PPI) network was conducted by the Search Tool for Retrieval of Interacting Genes (STRING).

Development and Evaluation of the Necroptosis-Related Prognostic Index

Based on the differentially expressed necroptosis-related genes with prognostic value, we carried out the least absolute shrinkage and selection operator (Lasso) with 10-fold cross-validation. Lastly, the coefficients and the penalty parameter (λ) were determined by the minimum criterion. The formula to calculate the necroptosis-related prognostic index (NRPI) was as follows: NRPI $= \sum_i \beta iSi$ (β: coefficients, S: gene expression level). The receiver operating characteristics (ROC) curves were used to evaluate the sensitivity and specificity of NPRI. Survival curves were plotted by Kaplan-Meier analysis to assess the overall survival of KIRC patients. Univariate and multivariate Cox regression analyses were performed to determine independent prognostic factors. These R software packages include *timeROC, survival, and survminer.*

Functional Enrichment Analysis

Gene Ontology (GO) and the Kyoto Encyclopedia of Genes and Genomes (KEGG) analyses were used to detect the potential biological mechanisms by the *clusterProfiler* R package. Gene set enrichment analysis (GSEA) was utilized to analyze the different NRPI subgroups with GSEA software 4.0.3.

Immune Cell Infiltration and Response to Immune Checkpoint Therapy

The stromal scores, immune scores, ESTIMATE scores, and tumor purity were calculated by the ESTIMATE algorithm. The algorithms including EPIC, XCELL, MCPCOUNTER, QUANTISEQ, CIBERSORT-ABS, CIBERSORT, and TIMER were carried out to explore the immune cell infiltration. The immune function was analyzed by single-sample gene set enrichment (ssGSEA). The process was performed using the R *GSVA, limma, GSEABase, ggpubr*, and *reshape2* packages.

The Application of NRPI in the Medical Treatment

We adopted the *ggpubr* package to investigate the relationship between the expressions of immune checkpoint and NRPI. We evaluated the half-maximal inhibitory concentration (IC50) of targeted drugs between the two NRPI subgroups. The R packages used here were *pRRophetic* and *ggplot2*.

Immunohistochemical Staining

A total of five paired KIRC and adjacent non-tumor tissues were collected from the Second People's Hospital of Foshan. The detailed clinicopathological information of patients was documented in Supplementary Table 1. Immunohistochemistry (IHC) staining was performed according to the instructions of the IHC kit (UltraSensitive™ SP, MX Biotechnologies, China; Cat. No: KIT-9730). The antibodies, PLK1 (WL04381, Wanleibio, Shenyang, China), TERT (WL02685, Wanleibio, Shenyang, China), and KLF9 (bs-3644R, Bioss, Beijing, China), were used in the experiments. The type of antibody used in this study was polyclonal antibody for three genes and the hosts of the antibodies were all rabbits. The percentage of positively stained cells was calculated and classified as zero (0–5%), one (6–25%), two (26–50%), three (51–75%), and four (76–100%). The intensity of staining was classified as zero (negative), one (weak), two (moderate), and three (strong). Immunoreactivity score (IRS) was calculated by multiplying the staining percentage and intensity score. Two experienced pathologists independently assessed the immunohistochemical results without knowledge of the patient's clinicopathology and clinical outcome. Any inconsistencies were reviewed by the two pathologists together until a consensus was reached. A total of five representative fields were microscopically photographed and documented (magnification, x100, x400) using Leica, APERIO CS2 and the amount of positively stained sites was enumerated. The quantitative analysis of IHC was recorded in Supplementary Table 2.

Statistical Analysis

All statistical analyses were applied by R version 4.1.1 (Institute for Statistics and Mathematics, Vienna, Austria) and some related packages were applied to all statistical analyses. $P < 0.05$ was considered the significantly statistical difference.

Result
The Differentially Expressed Necroptosis-Related Genes in KRIC

Figure 1 documented the total workflow of the study. A total of 53 necroptosis-related genes were found to be differentially expressed in 539 KIRC samples and 72 normal tissues from the TCGA database. (Figure 2A) To further screen out those with prognostic values, we identified 25 genes by univariate Cox regression analysis and Venn diagram. (Figure 2B and C) The PPI and correlation networks of these genes illustrated their close interactions and relationships. (Figure 2D and E) Following this, we used GO and KEGG pathway analyses to analyze the differentially expressed genes (DEGs). GO analysis revealed that these genes were mainly involved in extrinsic apoptotic signaling pathway, necrotic cell death, and death receptor. (Figure 2F) KEGG analysis suggested that these genes were closely related to TNF signaling pathway and cell death including necroptosis and apoptosis (Figure 2G).

Construction and Validation of NRPI

We performed univariate Cox regression and Lasso regression analyses on the 25 genes obtained above and finally constructed an NRPI consisting of 3 genes (PLK1, TERT, and KLF9) in the training set. (Figure 3A and B) Subsequently, using the median NRPI as the cut-off, we found that as the NRPI score increased, KIRC patients had more fatal events
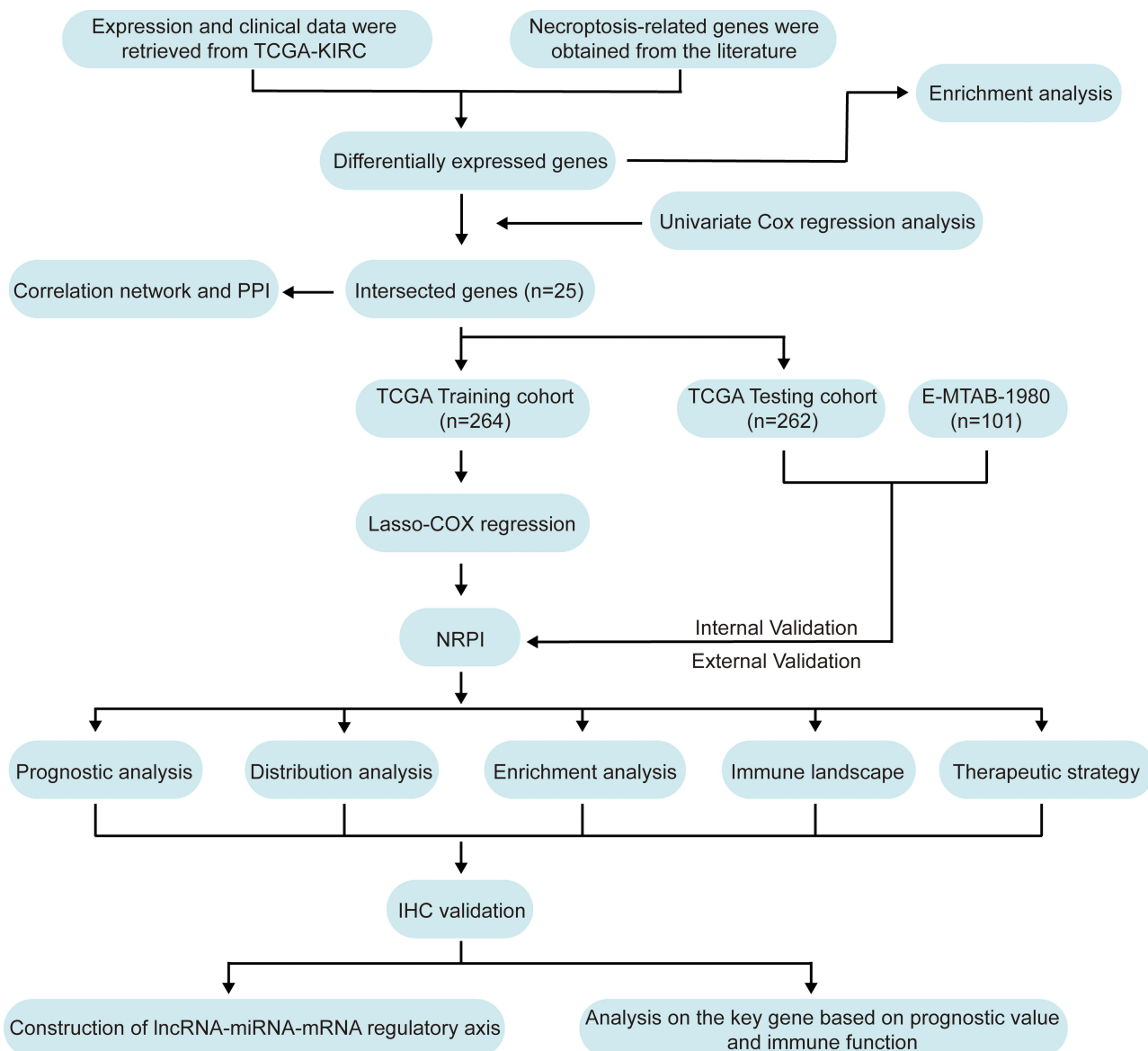
Figure 1 The workflow of this study.

and NRPI-high patients had worse overall survival than NRPI-low patients. (Figure 3C and D) The ROC analysis suggested that NRPI had good predictive accuracy. The area under curve (AUC) values of NRPI were 0.715 at 1 year, 0.680 at 2 years, and 0.676 at 3 years. (Figure 3E) Univariate and multivariate regression analyses further indicated that NRPI was an independent prognostic factor in KIRC (Figure 3F and G).

We validated the role of NRPI in the internal validation set, entire set, and external validation set. Consistent with the previous results, NRPI-high patients suffered a worse prognosis (P < 0.001). (Figure 4A–C) Meanwhile, NRPI could act as an independent prognostic factor, demonstrating good sensitivity and specificity in all three sets. (Figure 4D–I) Taken together, NRPI was an independent and reliable predictor in KIRC.

The Relationship Between Clinical Features and NRPI

There were significant distributional differences in the clinical features including survival status, N stage, M stage, T stage, tumor stage, tumor grade, and gender between both NRPI subgroups. (Figure 5A) The NRPI-high subgroup was significantly associated with male, high mortality, high-grade, and advanced-stage disease progression. (Figure 5B–H) After further
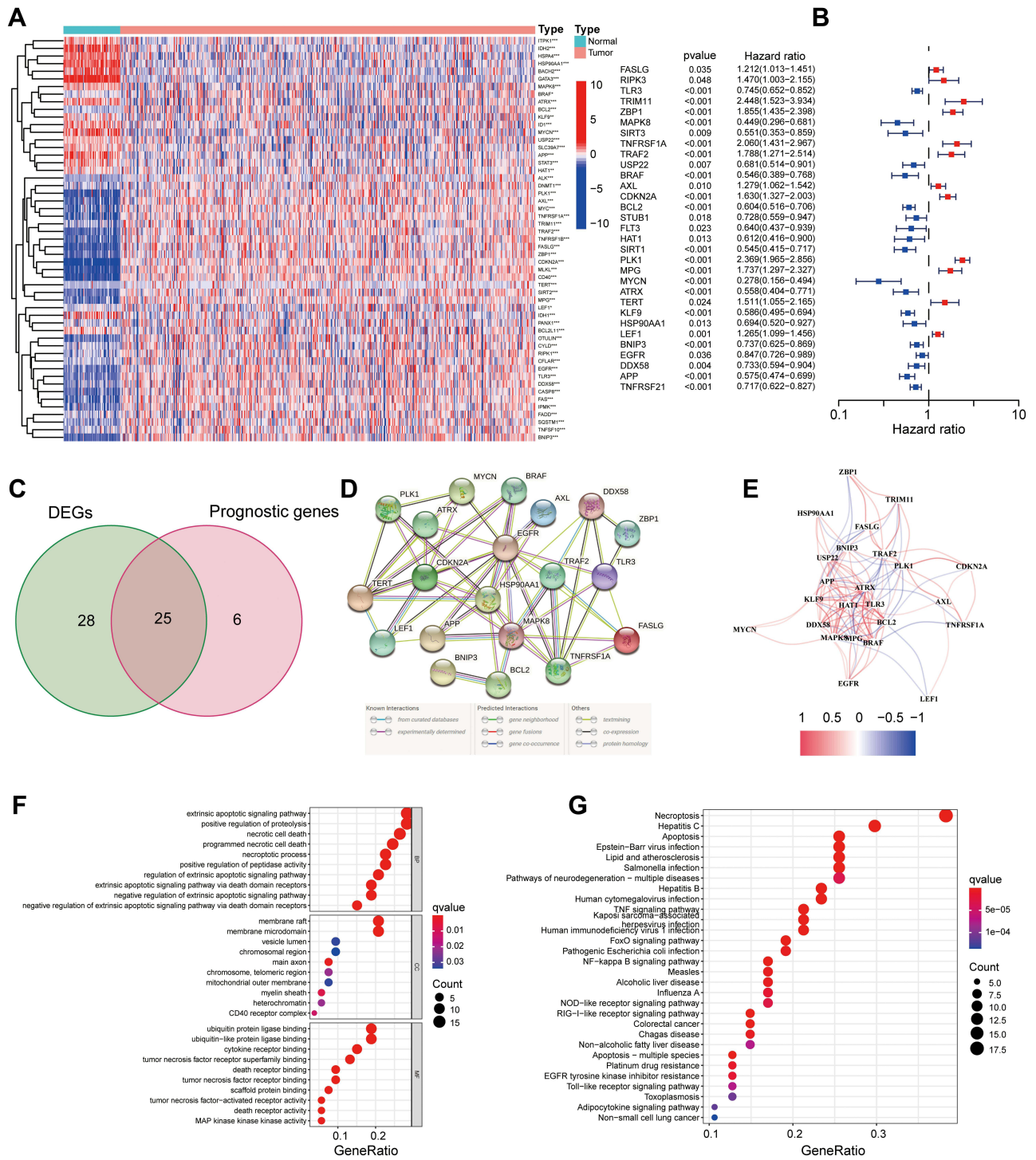
Figure 2 Screening out DEGs and their correlation in KIRC. (**A**) Differentially expressed necroptosis-related genes in tumor and normal tissues. (**B**) Univariate Cox regression analysis of prognostic genes. (**C**) Venn diagram of DEGs and prognostic genes (**D** and **E**) PPI network and correlation network of DEGs with prognostic value. (**F** and **G**) GO and KEGG analyses of DEGs. *P< 0.05, **P< 0.01, and ***P< 0.001.
Abbreviations: DEGs, differentially expressed genes; KIRC, kidney renal clear cell carcinoma; PPI, protein-protein interaction; GO, Gene Ontology; KEGG, Kyoto Encyclopedia of Genes and Genomes.

survival analysis of subgroups of KIRC patients with different ages, genders, and disease processes, we found that the NRPI-high subgroup was consistently in a worse prognosis. (Figure 5I) NRPI was closely related to clinical characteristics and remained a good predictor of performance for KIRC patients at different periods of disease progression.
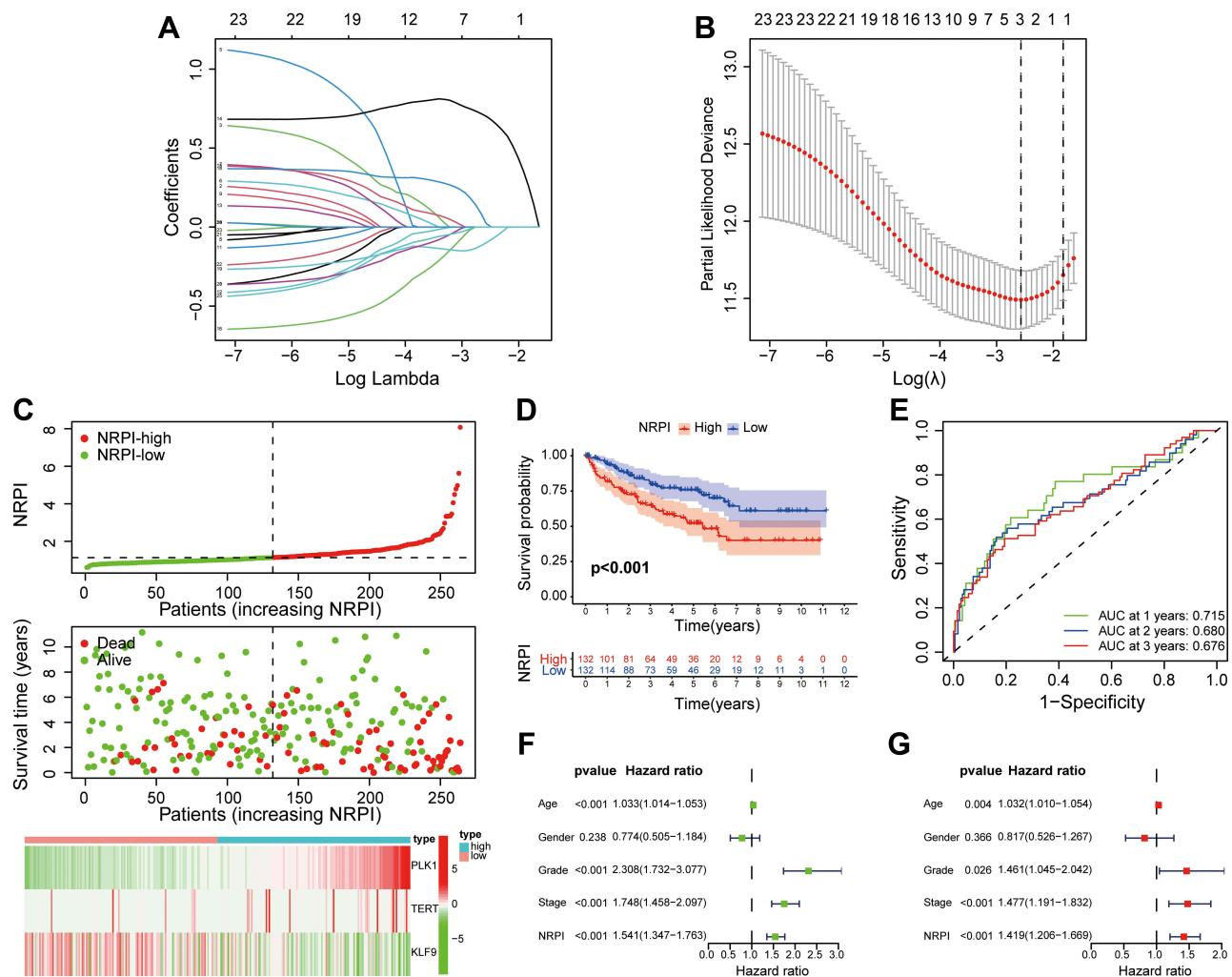
Figure 3 Construction of NRPI in KIRC. (**A**) LASSO coefficient expression profiles of candidate genes. (**B**) The penalty parameter (λ) in the LASSO model was selected through ten cross-validation. (**C**) The relationship between NRPI and survival time in the training cohort. (**D**) The Kaplan–Meier survival curve of the signature between two NRPI subgroups. (**E**) Time-dependent ROC curve analysis in the training cohort. (**F** and **G**) The univariate and multivariate Cox regression analyses in the training cohort.
Abbreviations: NRPI, necroptosis-related prognostic index; KIRC, kidney renal clear cell carcinoma; LASSO, least absolute shrinkage and selection operator; ROC, receiver operating characteristic.

Distribution Analysis and Construction of the Nomogram

The t-distributed Stochastic Neighbor Embedding (t-SNE) and 2D principal component analysis (PCA) analyses showed that the two subgroups exhibited two different distribution directions. (Figure 6A and B) 3D PCA based on three necroptosis-related genes showed that NRPI subgroups were in two different distribution patterns. (Figure 6C) However, PCA based on whole necroptosis-related genes and genome-wide expression profiles did not differ. (Figure 6D and E) Furthermore, to extend the prognostic power and clinical application of NRPI, we constructed a nomogram integrating age, grade, stage, and NRPI. (Figure 6F) 1-year, 2-year, and 3-year calibration curves reflected the agreement between the predicted and actual curves. (Figure 6G–I) Moreover, the AUC values and C-index were greater than the published signatures in KIRC.[8–10] (Figure 6J) Therefore, the NRPI-based nomogram was expected to have a good predictive power in clinical practice.

Biological Function and Pathway Analyses

We performed GO and KEGG analyses to clarify the biological processes and pathways involved in NRPI. Biological functions such as immune response-activating cell surface receptor signaling pathway, immune response-activating signal transduction, and neutrophil activation involved in immune response were associated with the NRPI. (Figure 7A) KEGG
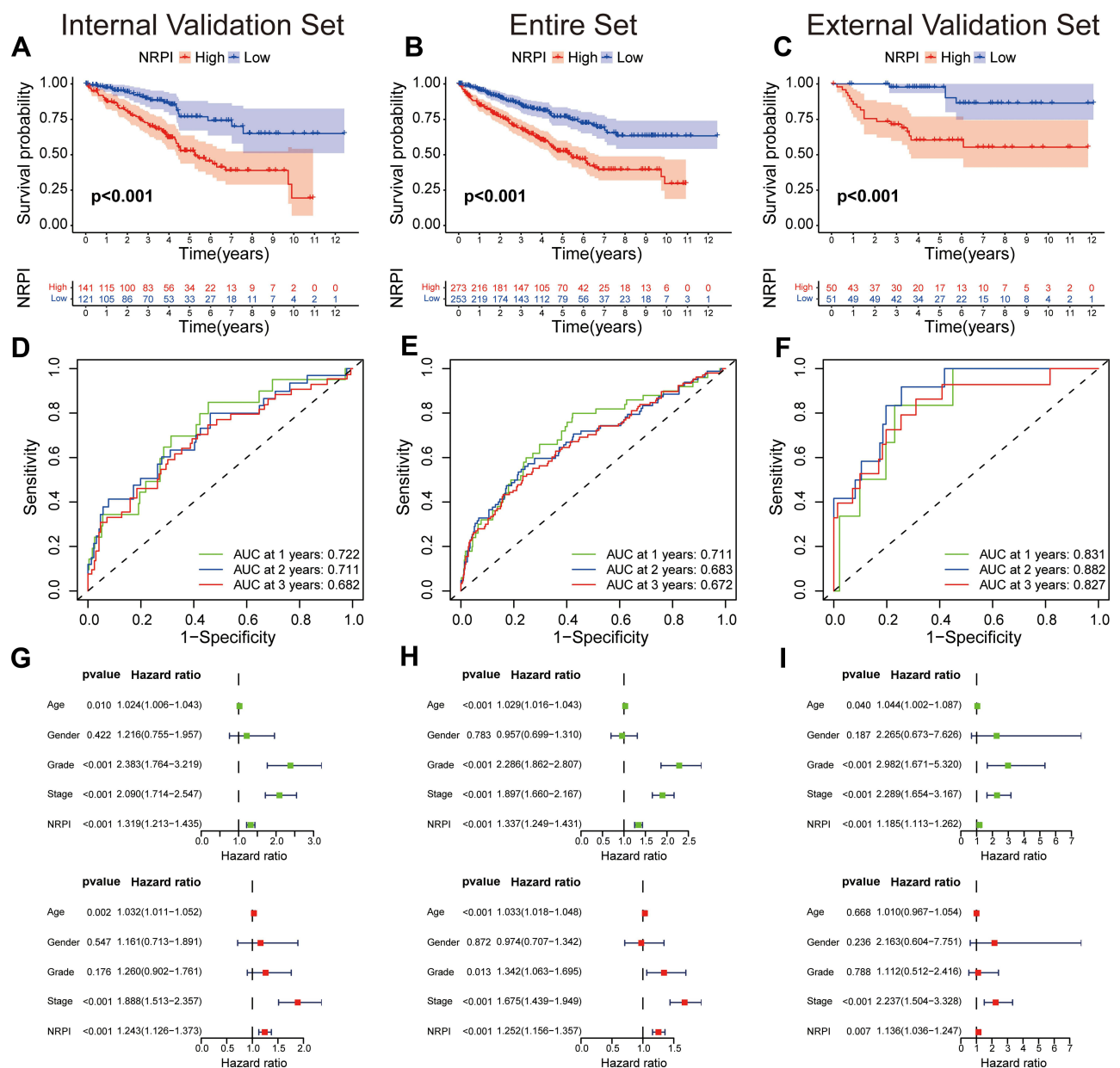
Figure 4 Validation of NRPI in multiple cohorts. Survival analyses in the (**A**) internal validation set, (**B**) entire set, and (**C**) external validation set. Time-dependent ROC curves analyses in the (**D**) internal validation set, (**E**) entire set, and (**F**) external validation set. The univariate and multivariate Cox regression analyses in the (**G**) internal validation set, (**H**) entire set, and (**I**) external validation set.
Abbreviations: NRPI, necroptosis-related prognostic index; ROC, receiver operating characteristic.

analysis showed that NRPI was involved in the PI3K-Akt signaling pathway and human papillomavirus infection. (Figure 7B) The GSEA indicated that the NRPI-high subgroup was significantly enriched items including regulation of T cell activation, B cell proliferation, cell cycle, and DNA replication. (Figure 7C) Collectively, this all suggested that there might be differences in immunobiology and immune infiltration in two NRPI subgroups, prompting us to further explore the implications of NPRI.

Correlation Between NRPI and Immune Infiltration

To better understand the tumor microenvironment, we found that the NRPI-high subgroup had higher immune scores, stromal scores, and ESTIMATE scores than the NRPI-low subgroup, indicating higher levels of immune cells in the tumor microenvironment of NRPI-high patients. (Figure 8A–E) Based on this, we further conducted multiple algorithms
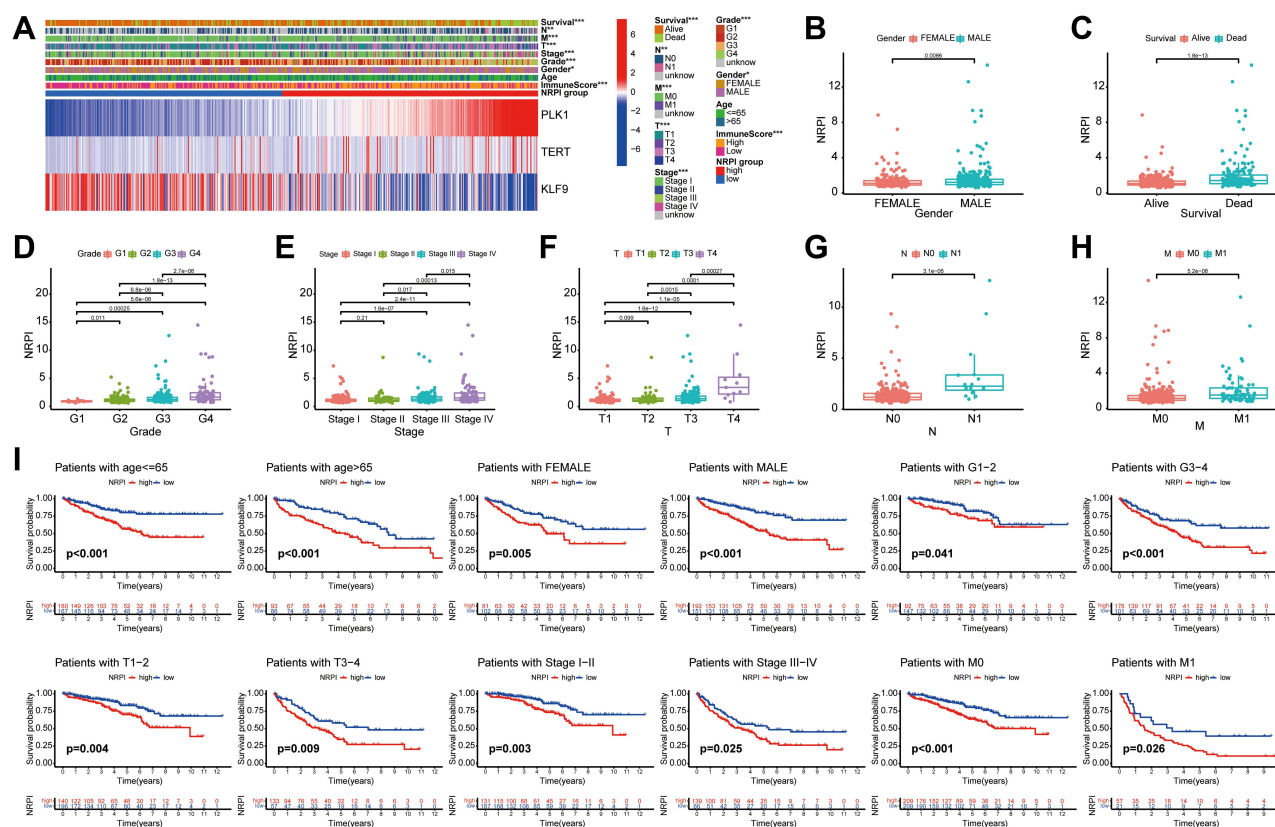
Figure 5 The relationship between NRPI and clinical factors. (**A**) The distribution of clinical factors between two NRPI subgroups. NRPI were significantly associated with (**B**) gender, (**C**) survival status, (**D**) grade, (**E**) stage, (**F**) T stage, (**G**) N stage, and (**H**) M stage. (**I**) Survival analyses in two subgroups stratified by different clinical features. *P< 0.05, **P< 0.01, and ***P< 0.001.

Abbreviation: NRPI, necroptosis-related prognostic index.

to explore the difference in immune cells infiltration in different NRPI subgroups. The heatmap depicted the presence of a variety of different infiltrating immune cell in the two NRPI subgroups, including CD8+ T cells, B cells, etc. (Figure 8F) There was a significant difference between different immune cells in the two NPRI subgroups, and these differences were relatively consistent across multiple algorithms. The ssGSEA algorithm revealed that the NRPI-high subgroup had a higher abundance of B cells, CD8+ T cells, macrophages, and regulatory T cells (Tregs) than the NRPI-low subgroup. (Figure 8G) Immune functions including CCR, checkpoint, cytolytic activity, human leukocyte antigen (HLA), and inflammation promoting likewise showed significant differences in different NRPI subgroups (Figure 8H).

The Application of NRPI in Medical Treatment

Immune checkpoints such as TIGIT, CTLA-4, and PD-1 were highly expressed in NRPI-high patients, and the same result was found for HLA expression. (Figure 9A and B) Tumor immune dysfunction and exclusion (TIDE) was used to assess the potential clinical efficacy of immunotherapy in different NRPI subgroups. NRPI-low patients had lower TIDE score and were more likely to benefit from immunotherapy than NRPI-high patients. (Figure 9C–E) Moreover, the AUC of NRPI was greater than that of TIDE and 18-gene T-cell-inflamed signature (TIS), implying a superior prognostic value for NRPI in KIRC. (Figure 9F) Sensitivity analysis of the commonly targeted drugs for KIRC treatment revealed that NRPI-high patients had higher sensitivity to sunitinib, pazopanib, rapamycin, and temsirolimus (Figure 9G–J).

The Expression Levels of Three Necroptosis-Related Genes in KIRC

In order to verify the expression levels of the three genes constituting NRPI in KIRC, we performed immunohistochemical staining on KIRC samples and adjacent non-tumor tissues from our hospital. The results showed that the expression
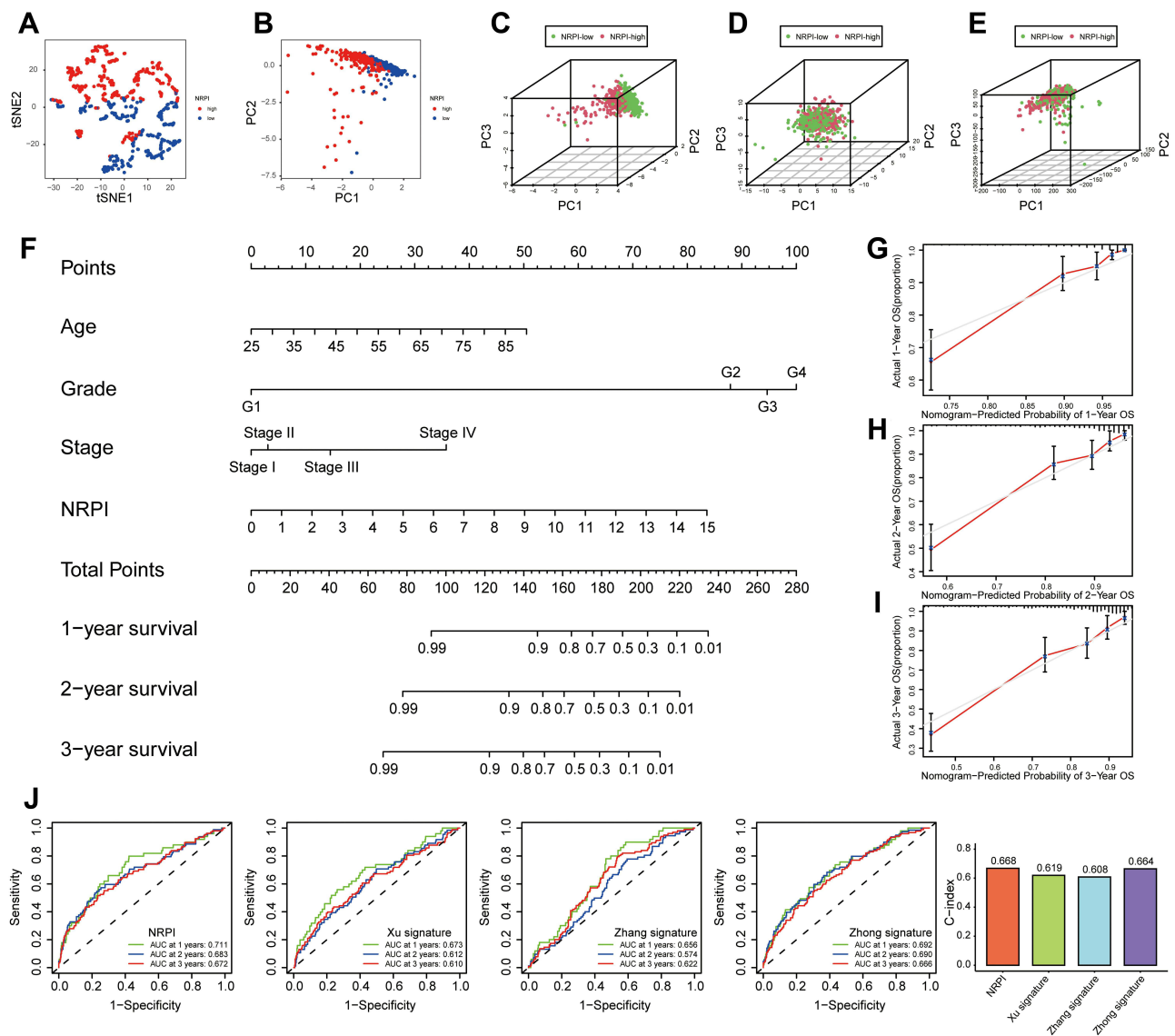
Figure 6 Distribution pattern and Construction of nomogram. (**A**) t-SNE analysis. (**B**) 2D PCA plot. 3D PCA based on (**C**) 3 necroptosis-related genes, (**D**) all necroptosis-related genes, (**E**) genome-wide expression profiles. (**F**) A nomogram integrating NRPI and clinicopathological variables predicts the 1-, 2-, and 3- year overall survival of KIRC patients. (**G-I**) Calibration curves for the validation of the nomogram. (**J**) The AUC values and C-index of NRPI and the three published signatures in KIRC.
Abbreviations: t-SNE, t-distributed stochastic neighbor embedding; PCA, principal component analysis; NRPI, necroptosis-related prognostic index; KIRC, kidney renal clear cell carcinoma; AUC, area under curve.

levels of PLK1 and TERT in KIRC were higher, while KLF9 was expressed at a lower level in KIRC. (Figure 10A) The mRNA expression of KIRC tissues and the corresponding normal tissues from TCGA were consistent with the immunoreactivity score derived from the results of IHC. (Figure 10B) Finally, we found that KIRC patients with high expression of PLK1 or low expression of KLF9 had shorter overall survival, while there was no statistically significant difference in the effect of different TERT expression on the survival of KIRC patients (Figure 10C).

Construction of a Network of lncRNA-miRNA-mRNA

As the previous results showed, PLK1 and KLF9 were significantly different in survival analysis, suggesting that these two genes may be involved in the process of tumor progression. Then we attempted to construct a lncRNA-miRNA-mRNA interaction network. Based on StarBase data, 124 miRNAs were identified as potential miRNA targets for KLF9. (Figure 11A) Under the criterion that the absolute value of the correlation coefficient was greater than 0.3, P value was less than 0.05, and the expression in the tumor was greater than that in normal tissues, only one miRNA entered our field of
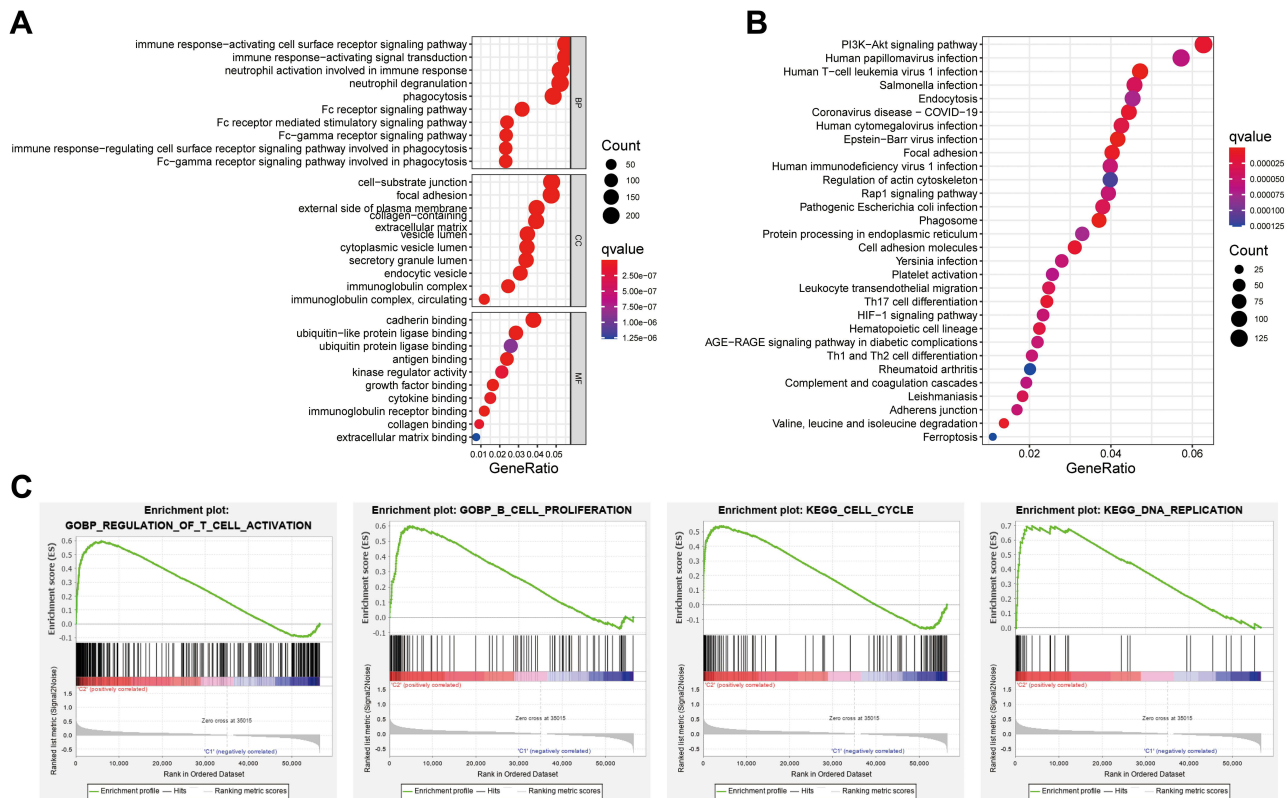
Figure 7 Functional analyses. (**A**) Go and (**B**) KEGG pathway analyses. (**C**) Enrichment plot by GSEA analysis.

vision, namely hsa-miR-21-5p. Under this criterion, PLK1 has no candidate targeted miRNA. Hsa-miR-21-5p, which is closely related to KLF9, was highly expressed in tumors and KIRC patients with high expression of hsa-miR-21-5p have a worse prognosis, suggesting that a negative regulatory relationship between KFL9 and hsa-miR-21-5p and that hsa-miR-21-5p influenced the malignant progression of tumors. (Figure 11B–D) Moreover, we further identified four upstream lncRNA targets OTUD6B-AS1, AL162377.1, AC108449.2, and AF111167.2 in StarBase (the inclusion criteria here were the absolute value of correlation coefficient > 0.3 and P < 0.05). (Figure 11E) They were all closely related to hsa-miR-21-5p. (Figure 11F) The prognosis of KIRC patients with their high expression levels was better. (Figure 11G) Therefore, we speculated that there was a negative regulatory relationship between lncRNAs and miRNA. The OTUD6B-AS1, AL162377.1, AC108449.2, and AF111167.2/hsa-miR-21-5p/KLF9 regulatory axis may play an important role in the progression of KIRC.

Validation of the Prognostic Value and Immune Function of KFL9 in KIRC

To further clarify the prognostic value of KLF9 in tumor tissues, we used univariate and multivariate Cox regression analyses to further demonstrate that KLF9 could be an independent prognostic factor in KIRC patients. (Figure 12A) Initially, our analysis revealed a close relationship between KLF9 and CD274 from the TIMER database. (Figure 12B) Next, we determined the strong relationship between KLF9 and immune cells including CD4+ T cells, mast cells, neutrophils, and myeloid dendritic cells. (Figure 12C) Some somatic cell copy number alterations in KIRC could suppress the level of immune cell infiltration (Figure 12D).

Discussion

KIRC is generally known to be a remarkably heterogeneous and aggressive malignancy.[11] Different clinical outcomes can still be found in patients with similar tumor stages or grades.[12] However, the existing clinical indicators and prognostic predictors are insufficient to meet the current clinical needs, and it is urgent to find a more accurate model to predict the prognosis of KIRC patients. Previous studies have shown that necroptosis played a complex and important
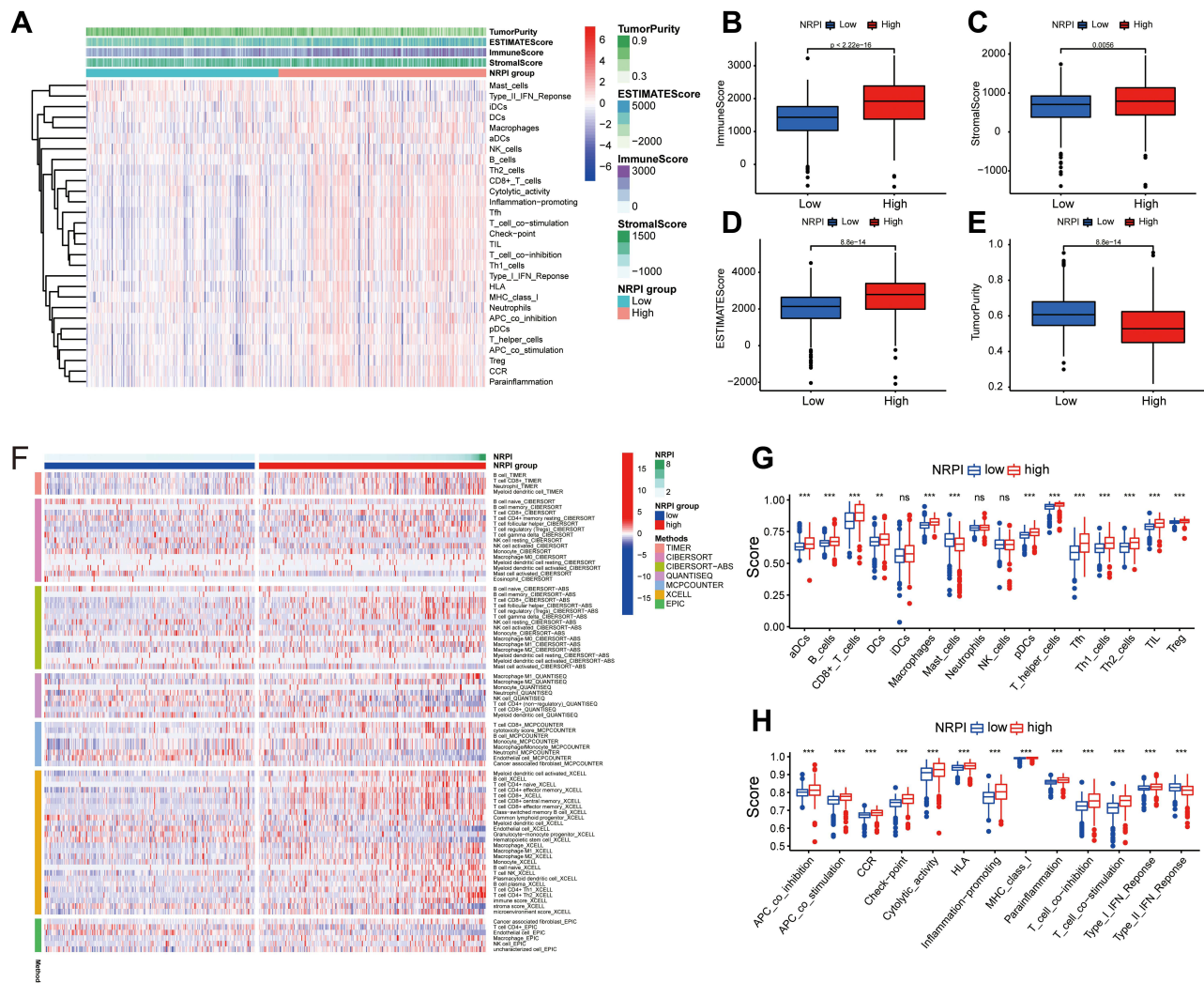
Figure 8 The immune cell infiltration and immune function. (**A**) Distribution of tumor purity, ESTIMATE score, immune score, and stromal score. The differences in (**B**) immune score, (**C**) stromal score, (**D**) ESTIMATE score, and (**E**) tumor purity between two NRPI subgroups. (**F**) The heatmap of immune cells in multiple algorithms. (**G**) Immune cell infiltration and (**H**) immune function were analyzed by ssGSEA algorithm. **P< 0.01 and ***P< 0.001.
Abbreviations: NRPI, necroptosis-related prognostic index; ssGSEA, single-sample gene set enrichment.

role in tumor initiation and progression.[13,14] Strilic et al[15] revealed that tumor cells could induce necroptosis in endothelial cells through activation of death receptor 6, thereby promoting tumor cell extravasation and tumor metastasis. Therefore, we expected to construct a prognostic model to meet the needs of the growing number of KIRC patients by using necroptosis as an entry point.

In our study, we first elucidated the differential expression of necroptosis-related genes in KIRC and normal kidney tissues, which led to the identification of 25 differentially expressed necroptosis-related genes with the prognostic value and further understanding of their relationship. Subsequently, we used Lasso Cox regression analysis to construct an NRPI, which was validated as an independent prognostic factor in multiple datasets. The NRPI was used to effectively group patients into NRPI-high and NRPI-low subgroups, which had very different prognoses and responses to treatment. NRPI-high had a worse prognosis and was more sensitive to targeted therapy, while NRPI-low patients responded better to immunotherapy. A more appropriate treatment could be chosen for KIRC patients through NRPI. At the same time, NRPI was closely correlated with clinical characteristics and was effective in predicting equally good performance in KIRC patients with different disease processes, demonstrating the broad applicability of NRPI. A comparison with three published signatures in KIRC revealed that NRPI had a better prediction accuracy. We also constructed a nomogram to
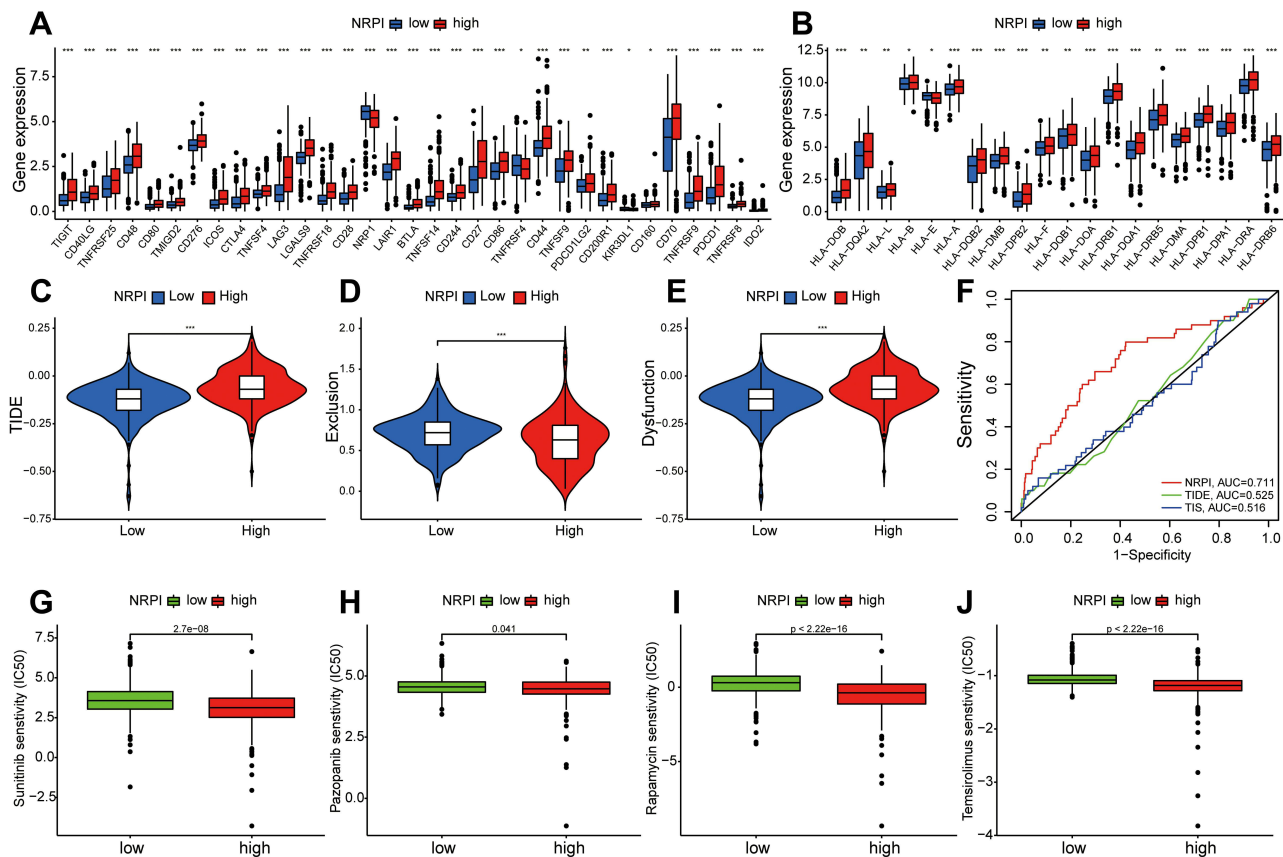
Figure 9 Application of NRPI in immunotherapy and targeted therapy. The expression of (**A**) immune checkpoints and (**B**) HLA between two NRPI subgroups. (**C-E**) Response to the immune checkpoint therapy by TIDE. (**F**) ROC analysis of NRPI, TIDE and TIS. (**G–J**) The sensitivity analysis of targeted therapy. *P< 0.05, **P< 0.01, and ***P< 0.001.

Abbreviations: NRPI, necroptosis-related prognostic index; HLA, human leukocyte antigen; TIDE, tumor immune dysfunction and exclusion; ROC, receiver operating characteristic; TIS, T-cell-inflamed signature.

predict 1-, 2-, and 3-year survival rates, increasing the clinical utility of the NRPI. Compared with a study that also used necroptosis-related genes to construct prognostic signature in KIRC,[16] our NPRI had higher predictive accuracy. Moreover, we further analyzed the prognostic outcomes of patients with various clinical stage and pathological grade. Compared with another study,[17] we used a smaller number of genes to construct a prognostic signature, which would be beneficial to clinical application and promotion, and also had higher clinical utility. Of importance, we not only analyzed the relationship between NPRI and the expression of immune checkpoints, but also performed TIDE analysis, which was currently recognized as an ideal method for predicting the efficacy of immunotherapy. The results showed that NRPI-low patients benefited more from immunotherapy. We further analyzed the relationship between NRPI and targeted therapy, which was a routine treatment for KIRC. Analyzing the sensitivity of targeted therapy was important for clinical treatment selection. Therefore, NPRI in our study was more reliable in predicting the prognosis of KIRC patients, and the role of NRPI in immunotherapy and targeted therapy was comprehensively explored, which might provide new ideas for the clinical treatment of KIRC.

NRPI was composed of three necroptosis-related genes (PLK1, TERT, KLF9). Polo-like kinase 1 (PLK1), a serine/ threonine kinase, regulates centrosome maturation and bipolar spindle formation, which is important for the process of mitosis.[18] A previous study has shown that PLK1 was upregulated in androgen-insensitive prostate cancer cells and could exert inhibitory effects to cause necrotic death.[19] In addition, PLK1 could mediate S369 phosphorylation of PIPK3 and thus regulate necrotic death.[20] PLK1 was considered as a marker of poor prognosis in KIRC.[21] It had been shown that PLK1 promoted the proliferation and invasion and inhibited apoptosis in renal cell carcinoma.[22,23] Telomerase reverse transcriptase (TERT) is overexpressed in 90% of malignant tumors and helps tumors maintain telomere length to obtain
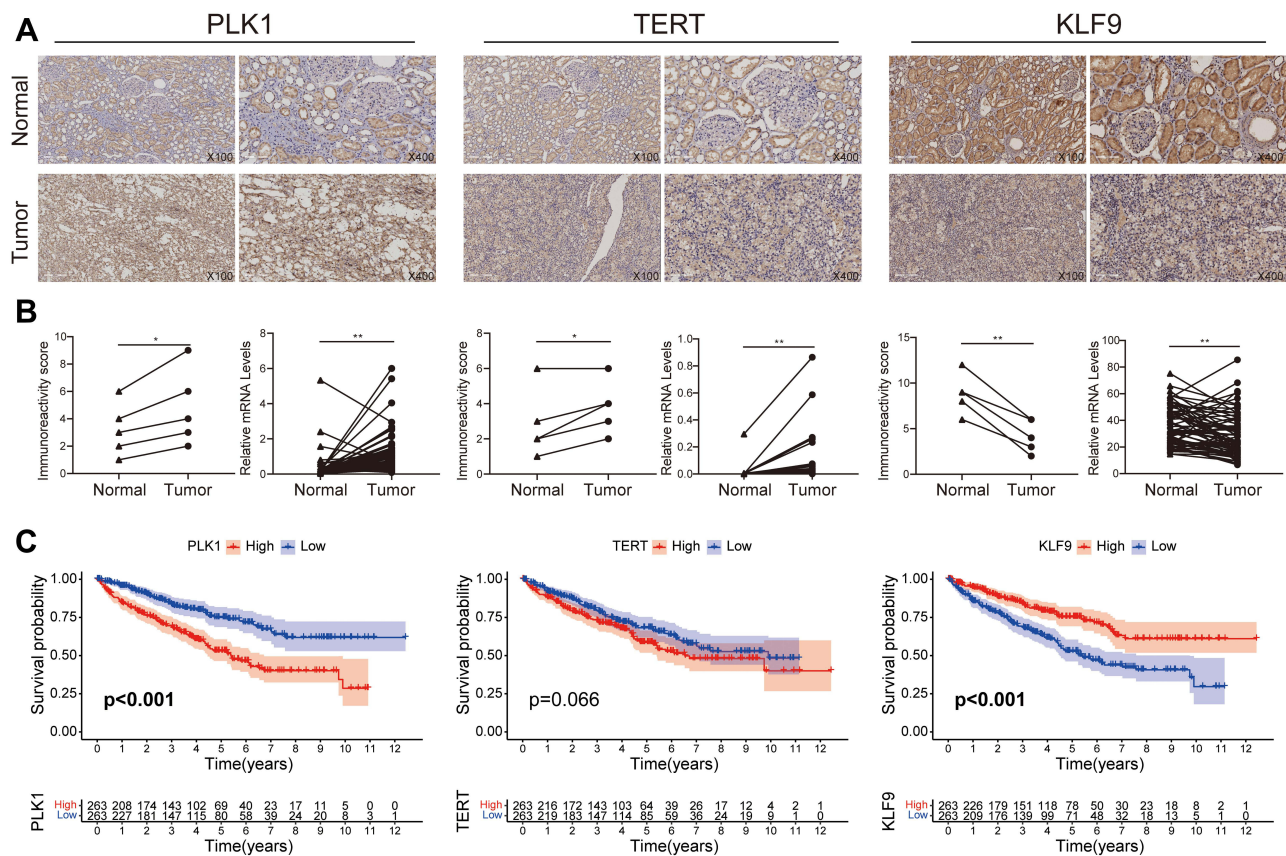
Figure 10 The expression of 3 necroptosis-related genes between KIRC and adjacent non-tumor tissues. (**A**) The protein expression analysis by IHC. (**B**) Immunoreactivity scores and mRNA levels from TCGA between tumor and normal issues. (**C**) Survival analyses of 3 necroptosis-related genes. *P< 0.05 and **P< 0.01.
Abbreviations: KIRC, kidney renal clear cell carcinoma; IHC, Immunohistochemistry; TCGA, the Cancer Genome Atlas.

immortal characteristics.[24] TERT could synergistically induce necroptosis in oral squamous cell carcinoma and inhibit tumor proliferation in vitro and in vivo.[25] TERT promoter mutations were associated with a poorer prognosis in KIRC.[26] Krueppel-like factor 9 (KLF9) is a member of the Sp1 C2H2-type zinc finger transcription factor family.[27] Tung et al discovered that KLF9 may cause cancer cell death through a mechanism of necroptosis, which may become a novel anti-tumor strategy for malignant brain tumors.[28] Low expression of KLF9 was associated with shortened overall survival in RCC patients.[29] In our IHC experiments, we perform protein-level validation on clinical KIRC and adjacent non-tumor samples from our hospital. Surprisingly, all three genes demonstrated significant disparities in KIRC and adjacent non-tumor samples. PLK1 and TERT had higher expression in KIRC than in adjacent non-tumor tissues. Conversely, KLF9 was highly expressed in non-tumor tissues, which was also consistent with the literatures that KLF9 was downregulated in expression in a number of cancers.[30,31]

Necroptosis is strongly associated with immunity and can play a role in the induction and amplification of cancer immunity. To maintain the role of peripheral T cell homeostasis, necroptosis can be achieved by eliminating excess T cells generated in antigen-induced T cell proliferation.[32] The immune-inflammatory cells which were generated during the process of necroptosis could promote angiogenesis, facilitating the proliferation and metastasis of cancer.[33] We turned our attention to the possibility that NRPI can influence the response of NRPI subgroups to immunotherapy through the immune landscape. Firstly, GO analysis suggested that NRPI may be closely related to multiple immunobiology. Further analysis revealed that the tumor microenvironment was also distinct in the two NRPI subgroups, with the NRPI-high subgroup having a higher immune score and lower tumor purity. The two subgroups also showed significant differences in immune cell infiltration. The different immune microenvironments may reflect different responses to immunotherapy. We used TIDE to predict the response of two subgroups to immunotherapy, which showed that the NRPI-low group was more likely to benefit from immunotherapy. We then compared NRPI with TIDE and TIS, two biological factors that
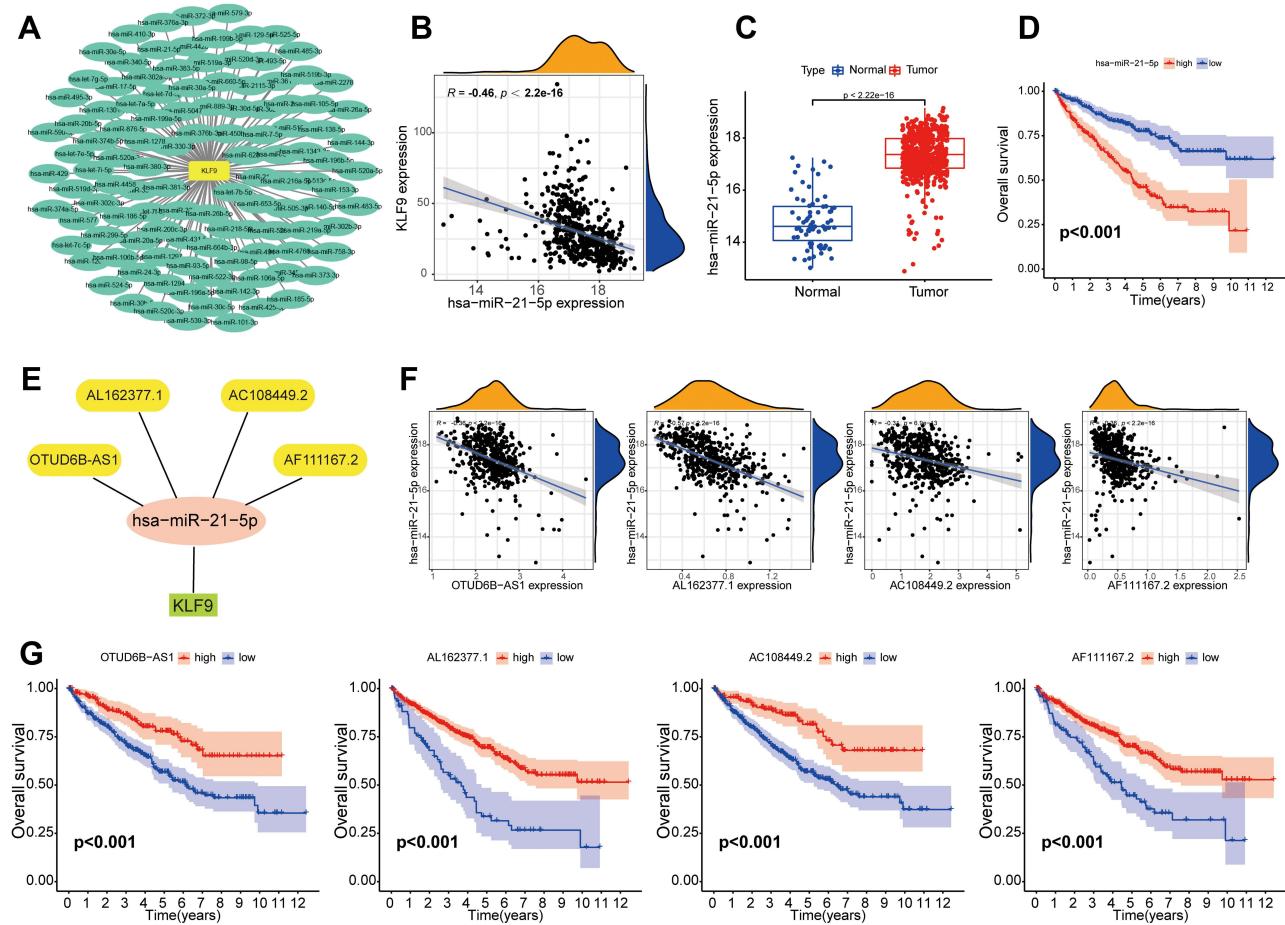
Figure 11 Construction of lncRNA-miRNA-mRNA regulatory axis. (**A**) The potential miRNAs target of KLF9. (**B**) The correlation between hsa-miR-21-5p and KLF9. (**C**) The expression of hsa-miR-21-5p between KIRC and normal tissues. (**D**) The survival analysis of hsa-miR-21-5p. (**E**) The lncRNA-miRNA-mRNA regulatory axis. (**F**) The correlation between hsa-miR-21-5p and lncRNAs. (**G**) The survival analysis of four lncRNAs in KIRC.
Abbreviations: KLF9, Krueppel-like factor 9; KIRC, kidney renal clear cell carcinoma.

predict response to immunotherapy. It was encouraging to see that NRPI was more accurate and specific in predicting patients' prognosis than TIDE and TIS. NRPI was composed of only three genes, which meant that it was more convenient for clinical testing than TIDE and TIS, and was not only a good predictor of immunotherapy, but also a more effective predictor of patients' prognosis.

Additionally, we constructed a OTUD6B-AS1, AL162377.1, AC108449.2, and AF111167.2/hsa-miR-21-5p/KLF9 regulatory axis for KIRC. The expression of OTUD6B-AS1, AL162377.1, AC108449.2, AF111167.2, hsa-miR-21-5p, and KLF9 affected the prognosis of KIRC patients. Previous reports indicated that high expression of hsa-miR-21-5p in six cancers including KIRC was strongly associated with shorter overall survival, which was consistent with our results.[34,35] In addition, hsa-miR-21-5p could drive T helper cells to participate in the kidney function and progression of IgA nephropathy.[36] Wang et al[37] found that high expression of LncRNA OTUD6B-AS1 represented a favorable prognosis and inhibited the proliferation and progression in KIRC. In our results, KLF9 was lowly expressed in tumors and closely associated with multiple immune cells and CD274. There might be a negative regulatory relationship between KLF9 and hsa-miR-21-5p. Similarly, LncRNA OTUD6B-AS1 might have a role in influencing the progression of KIRC by negatively regulating the high expression of hsa-miR-21-5p, which in turn affects the expression of KLF9. However, this result still needs to be validated in vitro and in vivo experiments.
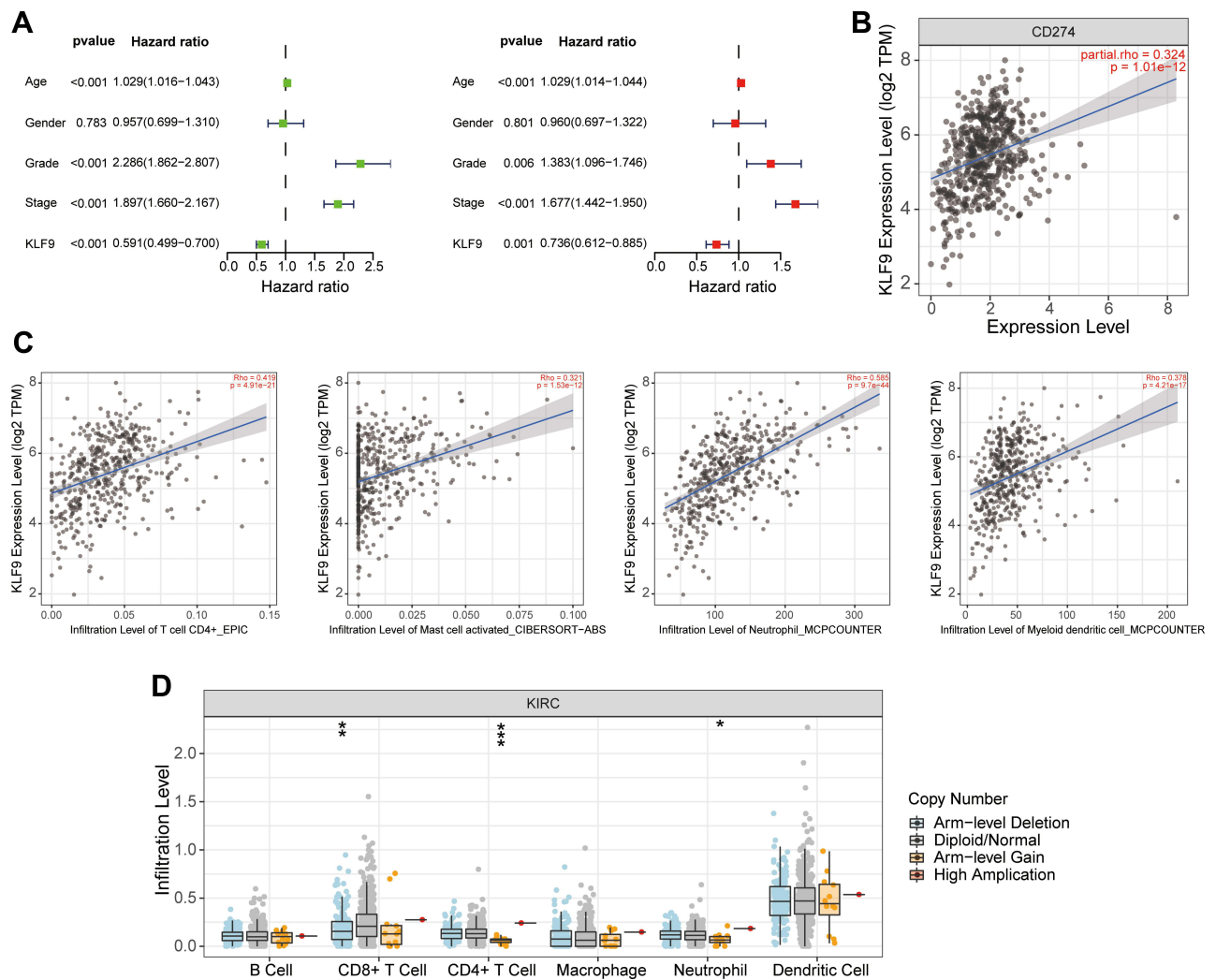
Figure 12 The prognostic and immune values of KLF9 in KIRC (**A**) The univariate and multivariate Cox regression analyses of KLF9. (**B**) The correlation between expression of KLF9 and CD274. (**C**) The correlation between expression of KLF9 and immune cells. (**D**) The correlation between copy number alteration of KLF9 and immune cells. *P< 0.05, **P< 0.01, and ***P< 0.001.

Abbreviations: KLF9, Krueppel-like factor 9; KIRC, kidney renal clear cell carcinoma.

Conclusion

In conclusion, NRPI was a promising necroptosis-related prognostic biomarker. NRPI could predict the prognosis and sensitivity to immunotherapy and targeted therapy in KIRC patients. We identified a OTUD6B-AS1, AL162377.1, AC108449.2, and AF111167.2/hsa-miR-21-5p/KLF9 regulatory axis for KIRC, but further studies were needed to fully elucidate.

Data Sharing Statement

All data generated or analyzed during this study are included in this published article.

Ethics Approval and Informed Consent

The research has been approved by ethics committee of the Second People's Hospital of Foshan. This study was conducted in accordance with the declaration of Helsinki. Informed consent was obtained from all individual participants included in the study.

Funding

No funds, grants, or other support was received.

Disclosure

The authors report no conflicts of interest in this work.

References

1. Sung H, Ferlay J, Siegel RL, et al. Global cancer statistics 2020: GLOBOCAN estimates of incidence and mortality worldwide for 36 cancers in 185 countries. *CA Cancer J Clin*. 2021;71:209–249. doi:10.3322/caac.21660

2. De P, Otterstatter MC, Semenciw R, Ellison LF, Marrett LD, Dryer D. Trends in incidence, mortality, and survival for kidney cancer in Canada, 1986–2007. *Cancer Causes Control*. 2014;25:1271–1281. doi:10.1007/s10552-014-0427-x

3. Howlander N, Noone A, Krapcho M, et al. SEER cancer statistics review, 1975-2016. *National Cancer Institute website*; 2019. Available from: seer.cancer.gov/csr/1975_2016/

4. Grootjans S, Vanden BT, Vandenabeele P. Initiation and execution mechanisms of necroptosis: an overview. *Cell Death Differ*. 2017;24:1184–1195. doi:10.1038/cdd.2017.65

5. Gong Y, Fan Z, Luo G, et al. The role of necroptosis in cancer biology and therapy. *Mol Cancer*. 2019;18:100. doi:10.1186/s12943-019-1029-8

6. Seehawer M, Heinzmann F, D'Artista L, et al. Necroptosis microenvironment directs lineage commitment in liver cancer. *Nature*. 2018;562:69–75. doi:10.1038/s41586-018-0519-y

7. Zhao Z, Liu H, Zhou X, et al. Necroptosis-related lncRNAs: predicting prognosis and the distinction between the cold and hot tumors in gastric cancer. *J Oncol*. 2021;2021:6718443. doi:10.1155/2021/6718443

8. Xu WH, Xu Y, Wang J, et al. Prognostic value and immune infiltration of novel signatures in clear cell renal cell carcinoma microenvironment. *Aging*. 2019;11:6999–7020. doi:10.18632/aging.102233

9. Zhang Z, Lin E, Zhuang H, et al. Construction of a novel gene-based model for prognosis prediction of clear cell renal cell carcinoma. *Cancer Cell Int*. 2020;20:27. doi:10.1186/s12935-020-1113-6

10. Zhong W, Huang C, Lin J, et al. Development and validation of nine-rna binding protein signature predicting overall survival for kidney renal clear cell carcinoma. *Front Genet*. 2020;11:568192. doi:10.3389/fgene.2020.568192

11. Czyzyk-Krzeska MF, Landero FJ, Gulati S, et al. Molecular and metabolic subtypes in sporadic and inherited clear cell renal cell carcinoma. *Genes*. 2021;12:388. doi:10.3390/genes12030388

12. Karam JA, Zhang XY, Tamboli P, et al. Development and characterization of clinically relevant tumor models from patients with renal cell carcinoma. *Eur Urol*. 2011;59:619–628. doi:10.1016/j.eururo.2010.11.043

13. Seifert L, Werba G, Tiwari S, et al. The necrosome promotes pancreatic oncogenesis via CXCL1 and Mincle-induced immune suppression. *Nature*. 2016;532:245–249. doi:10.1038/nature17403

14. Hanggi K, Vasilikos L, Valls AF, et al. RIPK1/RIPK3 promotes vascular permeability to allow tumor cell extravasation independent of its necroptotic function. *Cell Death Dis*. 2017;8:e2588. doi:10.1038/cddis.2017.20

15. Strilic B, Yang L, Albarran-Juarez J, et al. Tumour-cell-induced endothelial cell necroptosis via death receptor 6 promotes metastasis. *Nature*. 2016;536:215–218. doi:10.1038/nature19076

16. Chen W, Lin W, Wu L, Xu A, Liu C, Huang P. A novel prognostic predictor of immune microenvironment and therapeutic response in kidney renal clear cell carcinoma based on necroptosis-related gene signature. *Int J Med Sci*. 2022;19:377–392. doi:10.7150/ijms.69060

17. Xin S, Mao J, Duan C, et al. Identification and quantification of necroptosis landscape on therapy and prognosis in kidney renal clear cell carcinoma. *Front Genet*. 2022;13:832046. doi:10.3389/fgene.2022.832046

18. Barr FA, Sillje HH, Nigg EA. Polo-like kinases and the orchestration of cell division. *Nat Rev Mol Cell Biol*. 2004;5:429–440. doi:10.1038/nrm1401

19. Deeraksa A, Pan J, Sha Y, et al. Plk1 is upregulated in androgen-insensitive prostate cancer cells and its inhibition leads to necroptosis. *Oncogene*. 2013;32:2973–2983. doi:10.1038/onc.2012.309

20. Gupta K, Liu B. PLK1-mediated S369 phosphorylation of RIPK3 during G2 and M phases enables its ripoptosome incorporation and activity. *iScience*. 2021;24:102320. doi:10.1016/j.isci.2021.102320

21. Dufies M, Verbiest A, Cooley LS, et al. Plk1 upregulated by HIF-2, mediates metastasis and drug resistance of clear cell renal cell carcinoma. *Commun Biol*. 2021;4:166. doi:10.1038/s42003-021-01653-w

22. Gao Z, Man X, Li Z, et al. PLK1 promotes proliferation and suppresses apoptosis of renal cell carcinoma cells by phosphorylating MCM3. *Cancer Gene Ther*. 2020;27:412–423. doi:10.1038/s41417-019-0094-x

23. Zhang G, Zhang Z, Liu Z. Polo-like kinase 1 is overexpressed in renal cancer and participates in the proliferation and invasion of renal cancer cells. *Tumour Biol*. 2013;34:1887–1894. doi:10.1007/s13277-013-0732-0

24. Yu ST, Chen L, Wang HJ, Tang XD, Fang DC, Yang SM. hTERT promotes the invasion of telomerase-negative tumor cells in vitro. *Int J Oncol*. 2009;35:329–336.

25. Zhao X, Zhang C, Le Z, et al. Telomerase reverse transcriptase interference synergistically promotes tumor necrosis factor related apoptosis inducing ligand induced oral squamous cell carcinoma apoptosis and suppresses proliferation in vitro and in vivo. *Int J Mol Med*. 2018;42:1283–1294. doi:10.3892/ijmm.2018.3721

26. Casuscelli J, Becerra MF, Manley BJ, et al. Characterization and impact of TERT promoter region mutations on clinical outcome in renal cell carcinoma. *Eur Urol Focus*. 2019;5:642–649. doi:10.1016/j.euf.2017.09.008

27. Kikuchi Y, Sogawa K, Watanabe N, Kobayashi A, Fujii-Kuriyama Y. Purification and characterization of the DNA-binding domain of BTEB, a GC box-binding transcription factor, expressed in Escherichia coli. *J Biochem*. 1996;119:309–313. doi:10.1093/oxfordjournals.jbchem.a021240

28. Tung B, Ma D, Wang S, et al. Kruppel-like factor 9 and histone deacetylase inhibitors synergistically induce cell death in glioblastoma stem-like cells. *BMC Cancer*. 2018;18:1025. doi:10.1186/s12885-018-4874-8

29. Huang C, Li J, Zhang X, et al. The miR-140-5p/KLF9/KCNQ1 axis promotes the progression of renal cell carcinoma. *FASEB J.* 2020;34:10623–10639. doi:10.1096/fj.202000088RR

30. Simmen FA, Su Y, Xiao R, Zeng Z, Simmen RC. The Kruppel-like factor 9 (KLF9) network in HEC-1-A endometrial carcinoma cells suggests the carcinogenic potential of dys-regulated KLF9 expression. *Reprod Biol Endocrinol.* 2008;6:41. doi:10.1186/1477-7827-6-41

31. Kang L, Lu B, Xu J, Hu H, Lai M. Downregulation of Kruppel-like factor 9 in human colorectal cancer. *Pathol Int.* 2008;58:334–338. doi:10.1111/j.1440-1827.2008.02233.x

32. Yatim N, Jusforgues-Saklani H, Orozco S, et al. RIPK1 and NF-kappaB signaling in dying cells determines cross-priming of CD8 (+) T cells. *Science.* 2015;350:328–334. doi:10.1126/science.aad0395

33. Grivennikov SI, Greten FR, Karin M. Immunity inflammation, and cancer. *Cell.* 2010;140:883–899. doi:10.1016/j.cell.2010.01.025

34. Kowalczyk AE, Krazinski BE, Godlewski J, et al. SATB1 is down-regulated in clear cell renal cell carcinoma and correlates with miR-21-5p overexpression and poor prognosis. *Cancer Genomics Proteomics.* 2016;13:209–217.

35. Kajdasz A, Majer W, Kluzek K, et al. Identification of RCC subtype-specific microRNAs-meta-analysis of high-throughput RCC tumor microRNA expression data. *Cancers.* 2021;13:548. doi:10.3390/cancers13030548

36. Xu BY, Meng SJ, Shi SF, et al. MicroRNA-21-5p participates in IgA nephropathy by driving T helper cell polarization. *J Nephrol.* 2020;33:551–560. doi:10.1007/s40620-019-00682-3

37. Wang G, Zhang ZJ, Jian WG, et al. Novel long noncoding RNA OTUD6B-AS1 indicates poor prognosis and inhibits clear cell renal cell carcinoma proliferation via the Wnt/beta-catenin signaling pathway. *Mol Cancer.* 2019;18:15. doi:10.1186/s12943-019-0942-1